P8.13 ELECTRICAL CONDUCTIVITY OF SUPERCOOLED CLOUD WATER AT MT. WASHINGTON, NH

Charles C. Ryerson*, George G. Koenig, Debra A. Meese, Joyce A. Nagle, and James H. Cragin
U.S. Army Corps of Engineers Engineer Research and Development Center
Cold Regions Research and Engineering Laboratory
Hanover, New Hampshire

1. INTRODUCTION

Despite sophisticated forecast tools and onboard ice protection hardware, inflight icing still claims lives. Icing is a most serious problem for general aviation aircraft, helicopters, and commuter aircraft that fly low and slow and are potentially exposed to icing conditions more often than faster, higher-flying aircraft. Inflight deicing and anti-icing of aircraft wings and helicopter rotor blades is accomplished using two principal methods; by heating leading edge surfaces or by mechanically breaking ice away from the substrate. Thermal deicing and anti-icing is effective but consumes considerable power, especially during departure and approach when available power is limited and icing is most likely. The primary mechanical method is inflatable leading edge boots that expand causing ice to break and be carried away in the slip stream (FAA Icing Handbook, 1991). Deicing boots cause occasional aerodynamic penalties because of the need to accumulate ice before shedding, and because of residual ice that remains after the boots are deflated.

Petrenko (Petrenko, 1998; Petrenko and Qi 1999) discovered that application of a low voltage direct current to ice at an interface comprised of a fine matrix of conductors (cathodes and anodes 100 µm wide each, and separated by 100 µm wide insulators) will cause electrolysis to erode ice at the ice-substrate interface (Petrenko and Courville, 2000). Erosion of the ice creates hydrogen and oxygen bubbles that decouple it from the substrate.

The Petrenko electrolysis deicing technique has potential application to aircraft deicing, but the effectiveness of the method is dependent upon the conductivity of the ice that forms on the substrate, which is dependent upon the conductivity of the water that creates the ice.

The conductivity of ice varies with the chemically-induced ion content of the water, and is about one-third that of the conductivity of the liquid water from which it freezes. For example, water with only a 0.1% salt content has an electrical conductivity of 1839 µS cm^{-1} (the Siemens is an SI derived unit of measurement for electric conductance, being the inverse of ohm, and is the ratio of the current density to the electric field strength) whereas a sample of atmospheric water sampled at Mt. Washington, NH, through several storms in April 1999, had an average conductivity of 10.1 µS cm^{-1}. The result is that larger currents must be applied to low conductivity ice to cause electrolysis, and conductors must be closely spaced. Therefore, the design of a system that could utilize electrolysis deicing methods on aircraft, or on any iced structure, will be controlled by the electrical conductivity of the ice.

The objectives of this paper are to characterize the magnitude and variability of cloud water electrical conductivity and chemical composition at Mt. Washington Observatory (MWO) at the summit of Mt. Washington, NH. Source regions of air masses were backcast to assess causes of the conductivity measurements.

2. PREVIOUS STUDIES

In support of research to assess reasons for Red Spruce decline on Camel's Hump, VT, Hemmerlein and Perkins (1993) summarized seven cloud water events during the spring and summer of 1991. Water was collected on monofilament nylon strand collectors located above 550-m elevation (elevation not specified) on 1245-m Camel's Hump. Fifteen-minute averages of conductivity through 60.3 hours of measurements showed conductivity to vary between 74 µS cm^{-1} and 997 µS cm^{-1}, with event averages varying between 297 µS cm^{-1} and 994 µS cm^{-1}. As part of a comprehensive study of the relationships between mixed-phase cloud physical and chemical properties, Borys et al. (1988) measured the conductivity of cloud supercooled water in three events over a period of three days

---

* Corresponding author address: Charles C. Ryerson, ERDC-CRREL, 72 Lyme Rd., Hanover, NH 03755-1290

at Storm Peak Laboratory at the summit of 3220-m Mt. Werner in northwestern Colorado. Sample conductivity was reported to ±5% uncertainly for three events using a conductivity bridge and probe corrected to 25°C (electrical current flow increases with increasing temperature therefore conductivity is corrected to a standard temperature of 25°C). Conductivities ranged from 10-45 µS cm^{-1} in mixed-phase and liquid drop events.

Anderson et al. (1999) determined the conductivity of cloud water at the summit of Whiteface Mountain, NY at 1483 m, Whitetop Mountain, VA at 1686 m, and Clingman's Dome, TN at 2029 m. In general, cloud water conductivity increased with increasing altitude and with decreasing latitude. Over four summers conductivity at the summit of Whiteface Mountain averaged 129.59 µS cm^{-1} in 2049 samples, and over four summers and 1496 samples at Whitetop Mountain conductivity averaged 155.58 µS cm^{-1}. The conductivity of 600 samples averaged 199.74 µS cm^{-1} over three summers at Clingman's Dome.

Cini et al. (2002) collected cloud water at a mountainside site at an altitude of 950 m in the Tuscan Apennines of central Italy from November 1992 to March 1995. Cloud water was collected using a Teflon stranded collector. Conductivities ranged from 47 to 485.30 µS cm^{-1} in 20 samples yielding an average of 173.63 µS cm^{-1}. In general, the authors claimed that higher liquid water content equated to a lower conductivity, similar to the relationship in the eastern United States observed by Anderson et al. (1999).

We do not report on the conductivity of precipitation. Though Anderson et al. (1999) indicate that cloud water is 5 to 20 times more acidic than rain water, there is no direct evidence that the same relationship holds for conductivity.

3. DATA COLLECTION

We conducted field campaigns at the MWO to collect ice deposited on either non-metallic multi-cylinders or extruded acrylic rods from the impact of supercooled cloud droplets. Data from four winters (1987-1988, 1988-1989, 2000-2001, and 2001-2002) were analyzed for conductivity and chemical composition.

3.1 Rotating Multicylinders

The measurements from the winters of 1987-1988 and 1988-1989 were acquired from ice collected at MWO using specially constructed rotating multicylinders; simple devices used for measuring the liquid water content and drop size spectra of supercooled clouds (Figure 1). They consist of a series of stacked cylinders with varying diameters such that droplet collection efficiency changes with cylinder diameter. Collection efficiency is the ratio of the mass of drops within the volume of air swept out by a cylinder to the mass of drops actually intercepted by the cylinder.

Figure 1. Rotating multicylinder exposed to cloud at MWO.

The winters of 1987-1988 and 1988-1989 data were collected on Plexiglas multicylinders to insure no chemical interaction between the multicylinder and the ice deposited on the cylinder. However, we have no record detailing how the multicylinders were handled when ice was collected in the 1988-1989 field campaign.

3.2 Extruded acrylic rod

Observations during the winters of 2000-2001 and 2001-2002 were made by exposing approximately 38-cm long by 2.54-cm diameter extruded acrylic rods to supercooled clouds (Figure 2). Unlike the multicylinder, which rotates at one rpm, the acrylic rods did not rotate, and the inexpensive Lucite rods made it possible to significantly increase the number of ice samples collected. Since ice typically accretes on one side of a stationary rod, it can potentially modify the collection efficiency. We believe, however, that this had no effect on chemical analyses because electrical conductivities from each diameter of the multicylinder were nearly identical to one another.

Maintaining the chemical integrity of samples in the high winds and turbulence of Mt. Washington was challenging. To ensure that data samples were not contaminated, special rod handling procedures were observed. New rods were cleaned with methanol to remove contaminants and rinsed with Milli-Q® water in a plastic bin. When dry, rods were heat-sealed, doubled bagged, and remained in their sealed bags until exposed to the icing atmosphere.


Figure 2. Sample rod with ice in sealed bag for transport from MWO to analysis lab at the University of New Hampshire.

Rods and collection bags were transported to the summit in sealed coolers and were placed in a freezer for cold soaking. Rods were exposed on the northwest corner of the MWO observation deck. Holders were moved about 30 meters to the east in northeast winds to allow for more effective ice collection during certain storm events.

Personnel wore standard Tyvek® clean suits and donned new clean gloves after exiting the observatory building. Rods remained within their plastic bags as they were attached to the mount, assuring that only the clean bag interior touched the ice collection surface. Once the rod was installed, the bag was discarded and a data collection log sheet was started.

Ice was collected until 2-cm thickness of rime or 1 cm of clear ice had accreted. A minimum of 1 cm of rime ice was necessary for chemical analysis. Collection was halted if the wind speed was above 31 ms^{-1} since results from previous years showed potential contamination from either collection difficulties or windblown particles. Clean suits and gloves were again donned to retrieve iced rods. As during rod installation, gloves were placed on hands only after exiting the observatory building to reduce the probability of ice contamination. A clean bag was placed over the iced rod before removing it from the mounting bracket. Special care was needed to not break rime ice from the rod, especially when high winds were buffeting the plastic bag, rod, and observer. Observers noted the amount of ice that had collected on each rod, and the sample was stored in a freezer until transported frozen to the University of New Hampshire (UNH) for analysis at the Climate Change Research Center.

4. DATA COLLECTION AND ANALYSIS

4.1 Winters of 1987-1988 and 1988-1989

Fifty-two ice samples were collected during twelve sampling runs on the special multicylinders during the winters of 1987-1988 and 1988-1989 (Table 1). Hydrogen ion concentration (col. 4), and electrical conductivity (col. 5), were computed from the pH (col. 3). Selected ice samples were analyzed to obtain the total electrical conductivity (col. 6). To extend the analysis, the ratio of the total electrical conductivity divided by the conductivity due to hydrogen ions was computed (col. 8) and averaged for periods of consistent wind direction (col. 9). A comparison of the electrical conductivity due to hydrogen ions (col. 5) and the total electrical conductivity (col. 6) indicates that about 70% of the total electrical conductivity is due mainly to the presence of hydrogen ions.

Each stage of the multicylinder collects drops from a different region of the cloud drop spectra. Comparison of the hydrogen ion conductivity as a function of the multicylinder stage number did not indicate any significant dependency of the conductivity on drop size. When averaged across the multicylinders of each sampling case in column 10, total conductivity ranged from 2.6 $\mu S\ cm^{-1}$ to 112.0 $\mu S\ cm^{-1}$. Average conductivity was 27.1 $\mu S\ cm^{-1}$.

4.2 WINTERS OF 2000-2001 AND 2001-2002

Samples taken during the winters of 2000-2001 and 2001-2002 were analyzed for total conductivity and major ions including chloride (Cl), sodium (Na), magnesium (Mg), potassium (K), calcium (Ca), ammonium (NH4) and nitrate (NO3). Meteorological parameters were extracted from the MWO weather log and included as part of the database associated with the ice conductivity research. Chemical analyses were completed for 202 winter of 2000-2001 samples, and 145 winter of 2001-2000 samples.

Table 1. Analysis of the 1987-1988 and 1988-1989 ice samples collected at MWO.

Date	Stage[1]	pH	H[3] μeq/L	Cond[2] from H μS cm^{-1}	Total Cond μS cm^{-1}	Wind Dir. Degrees	H/total	Avg ratio	Total Cond μS cm^{-1}
3/16/1988	1	4.42	38	13.3	21.8	225	1.64		21.8
	2	4.45	35	12.4	21.6	225	1.74	1.69	21.6
4/5/1988	1	4.25	56	19.7		247			29.4
	2	4.22	60	21.1		247			31.5
	3	4.28	52	18.4		247			27.4
	4	4.28	52	18.4		247			27.4
	5	4.24	58	20.1		247			30.0
4/9/1988	1	5.00	10	3.5		80			5.0
	2	4.84	14	5.1		80			7.3
	3	4.76	17	6.1		80			8.8
	4	4.81	15	5.4		80			7.8
	5	4.86	14	4.8		80			6.9
4/11/1988	1	4.77	17	5.9	8.7	0	1.47		8.7
	2	4.78	17	5.8	8.3	0	1.43		8.3
	3	4.75	18	6.2	8.9	0	1.44		8.9
	4	4.68	21	7.3	10.5	0	1.44		10.5
	5	4.68	21	7.3	10.4	0	1.42	1.44	10.4
4/17/1988	1	4.24	58	20.1	27.2	270	1.35		27.2
	2	4.22	60	21.1	27.6	270	1.31		27.6
	3	4.27	54	18.8	25.6	270	1.36		25.6
	4	4.23	59	20.6	27.6	270	1.34		27.6
	5	4.25	56	19.7	26.5	270	1.35	1.34	26.5
4/20/1988	1	4.33	47	16.4		270			22.0
	2	4.27	54	18.8		270			25.2
	3	4.31	49	17.1		270			22.9
	4	4.22	60	21.1		270			28.3
4/22/1988	1	4.77	17	5.9	7.8	304	1.32		7.8
	2	4.75	18	6.2	8.0	304	1.29		8.0
	3	4.80	16	5.5	7.3	304	1.33		7.3
	4	4.85	14	4.9	6.8	304	1.39		6.8
	5	4.84	14	5.1	6.9	304	1.35	1.34	6.9
5/26/1988	1	5.64	2.3	0.8		0			1.2
	2	5.03	9.3	3.3		0			4.8
	3	5.05	8.9	3.1		0			4.5
	4	5.07	8.5	3.0		0			4.3
	5	5.27	5.4	1.9		0			2.7
6/10/1988	1	5.63	2.3	0.8		0			1.2
	2	5.26	5.5	1.9		0			2.7
	3	5.34	4.6	1.6		0			2.3
	4	5.18	6.6	2.3		0			3.3
	5	5.15	7.1	2.5		0			3.6
1/26/1989	1	3.67	214	74.8	108	180	1.44		108
	2	3.69	204	71.5	104	180	1.45		104
	3	3.64	229	80.2	124	180	1.55	1.48	124
3/17/1989	1	4.19	65	22.6		247			33.7
	2	4.19	65	22.6		247			33.7
	3	4.28	52	18.4		247			27.4

	4	4.36	44	15.3		247			22.8
3/18/1989	1	4.02	95	33.4		225			56.5
	2	4.01	98	34.2		225			57.8
	3	4.04	91	31.9		225			53.9
	4	4.07	85	29.8		225			50.4
	5	4.19	65	22.6		225			38.2

[1] Multicylinder stage. Stage 1 is smallest in diameter.

[2] Cond = conductivity.

[3] H = hydrogen

Table 2 shows the range of concentrations for each chemical species analyzed. The bottom row contains the percent variation between the mean concentrations of the two years. With the exception of Na and Cl, concentrations averaged higher the second year. However, the difference between Na and Cl for the two years is much smaller than for the other species. This may be a result of the trajectories of the storms sampled. Coastal storms cause higher concentrations of Na and Cl. Only a few coastal storms were sampled while the majority of the storms were of continental origin for this study (Climate Change Research Center, 1998). The table contains the maximum and minimum values for each species analyzed and the mean value.

Table 2. Analysis of the winter 2000-2001 and 2001-2002 ice samples collected at MWO.

2000-2001									
	Na (ppm)	**NH4 (ppm)**	**K (ppm)**	**Mg (ppm)**	**Ca (ppm)**	**Cl (ppm)**	**NO3 (ppm)**	**SO4 (ppm)**	**Conductivity (μS cm^{-1})**
Minimum	0	0	0	0	0	0	0	0	0.99
Maximum	15018	4914	608	1967	13698	12255	85974	31992	160
Mean	477	766	51	41	300	528	3566	3413	34
2001-2002									
Minimum	1.63	2.52	1.17	1.14	4.23	3.49	31	25	0.558
Maximum	9422	14080	1570	1639	14599	7964	61942	34483	444
Mean	385	1213	79	72	532	443	4818	4809	58
% Difference Yr2 - Yr1	-19	+37	+35	+43	+44	-16	+26	+29	+41

5. WIND DIRECTION ANALYSES

5.1 Winters of 1987-1988 and 1988-1989

When the original measurements were made at Mt. Washington during the winters of 1987-1988 and 1988-1989, meteorological data were not included as part of the data set. In order to backfill the wind direction (col. 7), information was obtained from the Air Force Combat Climate Center (AFCCC). Since the exact collection times of the ice samples were not recorded we subjectively determined the wind direction information from the information obtained from AFCCC. In most cases there was a prevailing wind direction for the entire day and it was not necessary to manipulate the wind direction information to derive a single value.

For those cases where wind direction changed during the day air parcel trajectories were subjectively determined using radiosonde information and 925-, 850-, 700-, and 500-millibar pressure level maps. Radiosonde flights and pressure maps at 00 UTC for days when ice samples were obtained provided a general idea of the flow pattern in the vicinity of Mt. Washington. For example, on March 18, 1989 the surface winds at Mt. Washington are from the southwest and the conductivity is the second highest recorded of all days sampled (the highest values are associated with winds from the south). The altitude of Mt. Washington is 1916 meters (approximately 800 mb). On the 850 mb (approximately 1500 meters) 3/18/1989 00Z pressure map (Figure 3) the flow over much of the northeast is from the southwest. The 00Z radiosonde (Figure 4) for this day from Chatham, MA (CHH) indicates the flow at the altitude of the summit of Mt. Washington is also from the southwest. In general, we anticipate flow from the southwest to contain more pollutants and potentially have higher acidity as the flow from the southwest crosses heavily industrialized and populated areas, allowing the air masses to incorporate pollutants as they cross these areas.

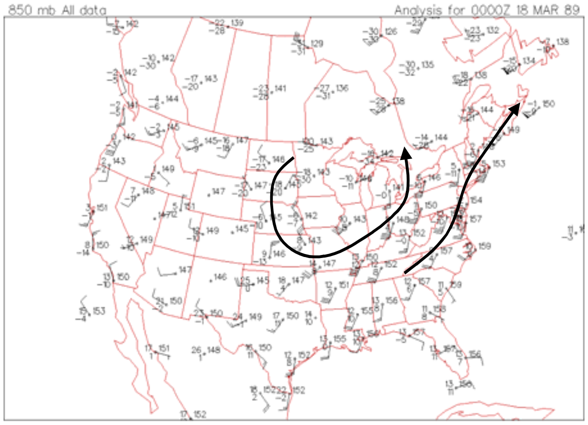

Figure 3. The 00Z 850 mb pressure map for 3/18/1989.

The most acidic samples (lowest pH values) are associated with winds from the south (Figure 5). Winds from the southwest also exhibit fairly high values of pH while winds from the north exhibit the lowest values of pH.

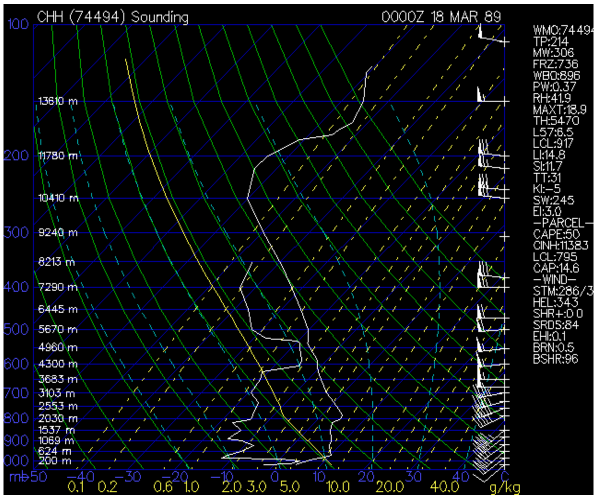

Figure 4. The 00Z radiosonde from Chatham, MA (CHH) for 3/18/1989.

5.2 Winters of 2000-2001 and 2001-2002

In order to determine if there was a relationship between the conductivity and the wind direction as recorded at the summit of Mt. Washington when ice samples were obtained it was necessary to analyze the data using a contingency table. This was required since the wind direction was recorded using a 15-degree interval in 2000-2001, and a 10-degree interval for 2001-2002. Wind directions in Figures 6 and 7 were categorized to allow construction of a frequency histogram. Conductivity is plotted as a function of the wind direction reported at the summit, but. since the conductivity is reported as a continuous variant it was necessary to recast the conductivity as a dichotomous variant. This was achieved by computing the average conductivity for the entire dataset for each year and then comparing the individual conductivity values with the appropriate average to determine if the individual values were greater than or less than the average. The interval used for each of the wind directions in Tables 3 and 4 was 45-degrees centered on the direction.

To test the null hypothesis that the rows in the contingency tables are independent of the columns, that is, the level of the conductivity relative to the average conductivity is independent of the wind direction, it is necessary to generate no-relation tables corresponding to each contingency table. The expected frequency for each element of the no-relation contingency table is obtained from

$$\textit{expected frequency for row(i), column(j)=}\quad \frac{\textit{[Column(j) total]x [row(i) total]}}{\textit{grand total}}$$

A chi-squared test is used to test for independence. The chi-squared test is computed as

$$\chi^2 = \sum_i \frac{(o_i - e_i)}{e_i}$$

where o_i is the observed frequency for the I^{th} cell and e_i is the expected frequency from the corresponding cell in the no-relation contingency

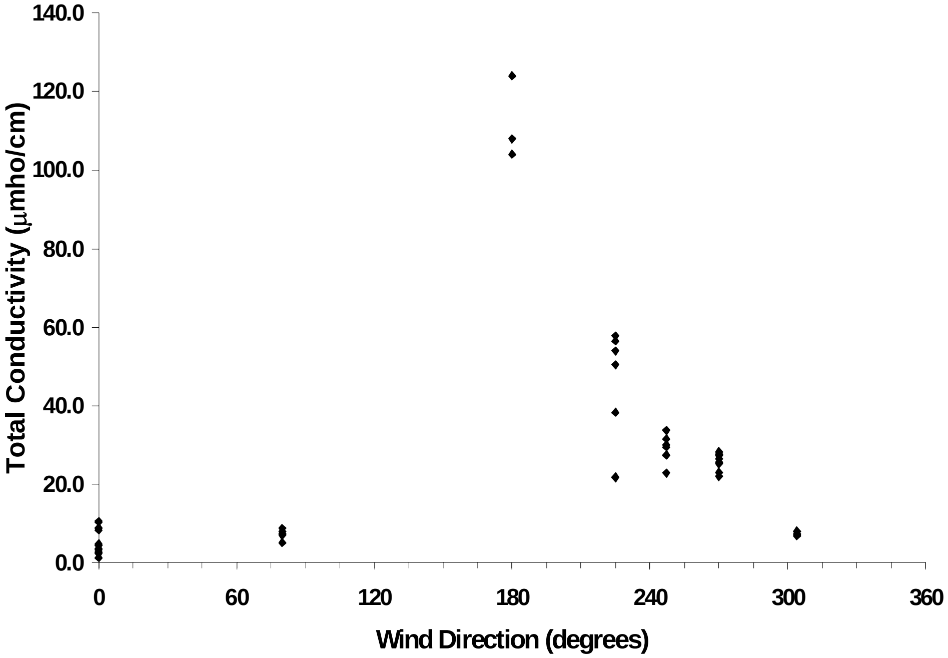

Figure 5. Total electrical conductivity vs. wind direction during the winters of 1987-1988 and 1988-1989.

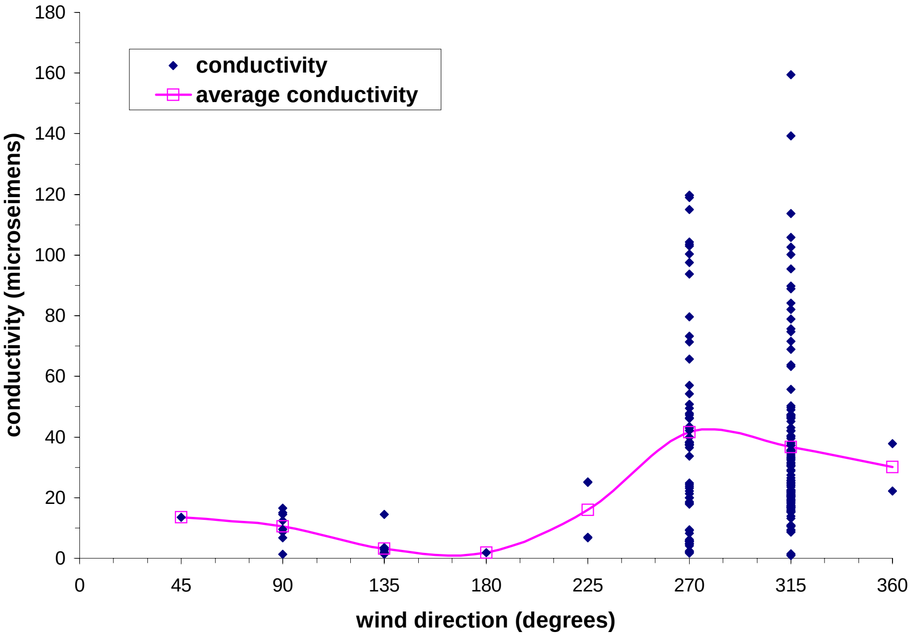

Figure 6. Conductivity vs. wind direction for the 2000-2001 ice samples.

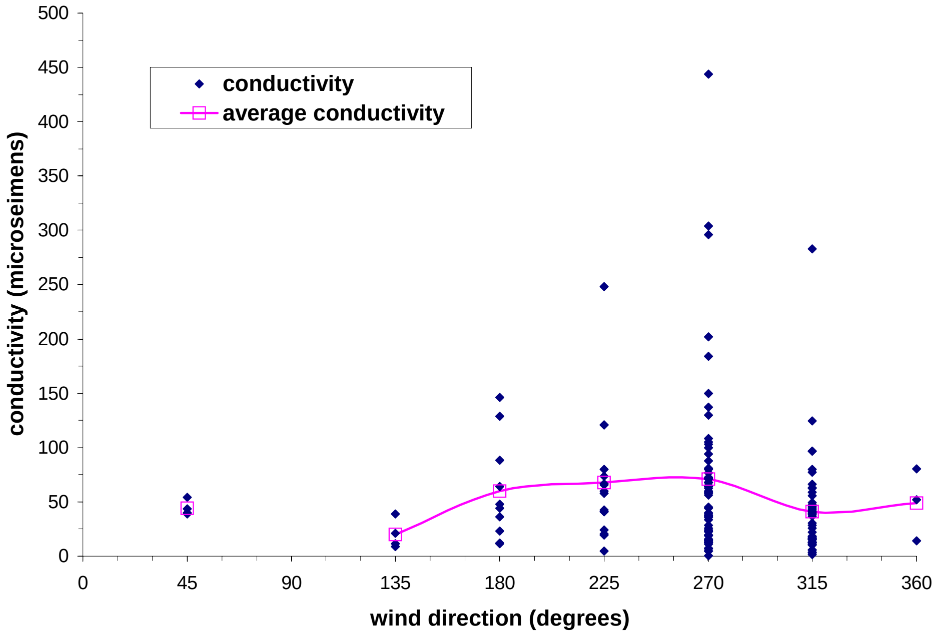

Figure 7. Conductivity vs. wind direction for the 2001-2002 ice samples.

Table 3. Contingency table for conductivity vs. wind direction analysis for the 2000-2001 data.

	N	**NE**	**E**	**SE**	**S**	**SW**	**W**	**NW**	**Total**
>Average	1	0	0	0	0	0	35	44	80
<= Average	1	1	8	12	1	4	28	67	122
Total	2	1	8	12	1	4	63	111	202
Average Conductivity (μS cm^{-1})	30.05	13.52	10.62	3.19	1.93	16.02	41.66	36.90	
Maximum Conductivity (μS cm^{-1})	37.86	13.52	16.64	14.52	1.93	25.17	119.80	159.50	

Table 4. Contingency table for conductivity vs. wind direction analysis for the 2001-2002 data.

	N	**NE**	**E**	**SE**	**S**	**SW**	**W**	**NW**	**Total**
>Average	1	0	0	0	3	9	29	12	54
<= Average	2	4	0	4	6	7	29	39	91
Total	3	4	0	4	9	16	58	51	145
Average Conductivity (μS cm^{-1})	48.87	44.20	No samples	20.09	59.84	67.95	70.73	41.21	
Maximum Conductivity (μS cm^{-1})	80.2	54.2	No Samples	38.8	146	248	443.5	283	

table. For $\chi^2 > \chi_\alpha^2$ with (number of rows-1) * (number of columns-1) degrees of freedom the null hypothesis is rejected at the α level of significance. For the 2000-2001 data set χ^2 was 24.003, while for the 2001-2002 dataset it was 23.73. For both datasets we can reject the null hypothesis at the 99% confidence level. That is, the rows (the conductivity relative to the overall average conductivity) are not independent of the columns (cardinal wind directions) used in the study. Since we had less than five samples for some wind directions care must be used in interpreting the results.

6. TRAJECTORY ANALYSES

The chemical composition and the total conductivity of the Mt. Washington ice samples reflect, in part, the history or trajectory of the supercooled liquid water arriving at the collection site. The emission sources over which an air mass passes, and the period of time the air mass is resident over an emission source, influence its properties when it arrives at Mt. Washington. Therefore, we computed air mass trajectories terminating at Mt. Washington on the day that ice was sampled, and integrated information regarding emission sources into the trajectory analysis, to assess their influence on the ice chemistry and conductivity.

Ninety-six hour backward trajectories were computed using NOAA's Hybrid Single-Particle Lagrangian Integrated (HYSPLIT-IV) model. HYSPLIT-IV computes trajectories, dispersion and deposition simulations using previously gridded meteorological data. A Lagrangian coordinate system moves with the flow the air parcel is embedded in. The trajectory is the time integration of the position of the air parcels as the three-dimensional wind field advects the parcel.

6.1 *Emission Databases*

A database containing estimates of annual emissions was compiled for point sources in the eastern US and Canada. The point sources were stationary sources of emissions, such as electric power plants or steel mills, which could be identified by name and location. Figure 8 represents all SO_2 sources in our database with an output of over 9.1×10^5 kg yr^{-1}.

6.1.1 US Data

Point source emissions data for the US portion of the study database were acquired from the US Environmental Protection Agency's (EPA) National Emission Trends (NET) Database (http://www.epa.gov/air/data/help/hnetemis.html). The NET database is an emissions inventory that contains estimates of annual emissions of criteria air pollutants from point, area, and mobile sources. The NET Database is released for point sources every three years (e.g., 1996, 1999, etc.) by the EPA and includes emissions estimates for all 50 states, the District of Columbia, Puerto Rico, and the Virgin Islands. In this study, only data from 1999 were used.

6.1.2 Canadian Data

A single source of point source data was not available for the Canadian portion of the study database. Consequently, data was collected from a search of Internet sources. Only point source data for SO_2 was available for Canadian point sources and the years of the data vary from 1997-2002.

Two primary sources of data were identified. First, under the Canadian/US Air Quality Agreement, Canada is obligated to notify the United States of any sites that would likely cause significant transboundary air pollution. The Transboundary Air Notifications (http://www2.ec.gc.ca/pdb/can_us/canus_trans_e.cfm) contain information for such locations within 100 km of the Canada-US border. Other point source data were compiled from annual reports of electric generating power plants, smelting operations, and paper mills. The US and Canadian databases were combined and all trajectory analyses used the entire database of point source emissions.

6.2 *Analysis of Trajectories and Emission Sources*

In the above analysis we used the wind direction as recorded by the observer when the samples were obtained, and an approximate trajectory analysis when summit winds were in question. These wind directions, however, do not necessarily reflect the actual trajectory of air parcels prior to arriving at Mt. Washington.

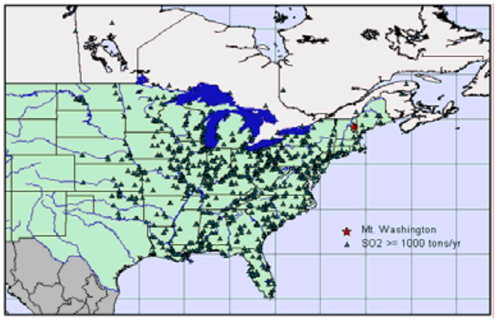

Figure 8. Location of all point sources with SO_2 greater than or equal to 9.1 x 10^5 kg $year^{-1}$.

6.2.1 *Winters of 2000-2001 and 2001-2002*

Based on the HYSPLIT-IV 96-hour trajectory information both the average (vector) wind direction and the most frequently occurring wind direction were computed for each trajectory. The average wind direction was then associated with the appropriate categorical wind directions. For example, an average wind direction of 280 degrees falls in the categorical direction denoted as 270 (West) degrees and covers the wind direction from 225 to 315 degrees. The most frequent wind direction was determined by assigning each one-hour segment of the trajectory to one of the eight categorical wind directions. The results for the average wind direction and the most frequent wind direction are similar and only the average wind direction analysis will be presented. In addition, several of the categorical wind directions did not have samples, or had less than 5 samples, therefore, the only analysis that will be presented will be graphical.

Sixty-six backward trajectories were calculated from Mt. Washington using the HYSPLIT-IV model. Each trajectory path was analyzed to determine the time of exposure to the point sources along the trajectory path. The back trajectories were calculated at one-hour intervals for up to 96 hours and were generated as a series of points containing the latitude/longitude and the time prior to the air parcel reaching Mt. Washington. Figure 9 shows the results for the trajectory analysis for 22 February 2002 predicted by HYSPLIT-IV. Figures 10 and 11 show the wind directions versus conductivity for the two winters as a result of the trajectory analyses. The trajectory analyses produced results similar to the analyses based upon wind directions measured at the summit (Figures 6 and 7),

The exposure time of air parcels to point sources was calculated by creating a 100-km radius circle (buffer) around each point source with emissions of SO_2 greater than or equal to 9.1 x 10^5 kg $year^{-1}$. The time the air parcel was within 100-km of a point source was calculated by determining the intersections of the projected trajectory path with the buffers and summing up the length of time the air parcel spent in each buffer.

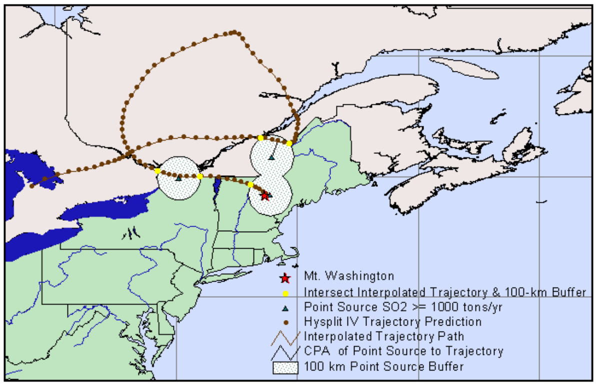

Figure 9. Predicted HYSPLIT-IV trajectory for 22 February 2002. The total time the air parcel was exposed to point source emissions of SO_2 greater than or equal to 9.1 x 10^5 kg $year^{-1}$ was 16 hours.

Aerosol samples from Odiorne Point, NH show distinct correlation with air masses from different regions. Marine air masses show high levels of the sea salt components sodium and chloride, air masses coming from the south or the eastern seaboard show high levels of acidic species indicating fossil fuel burning and those air masses from Canada show low sea salt, but high sulfate originating from the smelting of sulfur rich ores in the Sudbury region of Ontario. Air masses from the northwest also show high levels of ammonium, reflecting agricultural sources from the rural areas to the northwest of New Hampshire's sea coast. Rime-ice chemistry from Mt. Washington shows similar trends where a southwest trajectory out of the Ohio River Valley contained elevated concentrations of nitrate and sulfate reflecting emissions from coal and oil burning power plants and mobile sources in the Ohio River Valley. A west-northwest trajectory was coincident with a decrease in the concentration of nitrate and an increase in concentration of sulfate, perhaps reflecting anthropogenic sources in the Great Lakes industrial region and/or Sudbury, Ontario. This Canadian air mass also shows higher levels of ammonium, consistent with agricultural sources to the northwest of Mt. Washington (Climate Change Research Center, 1998).

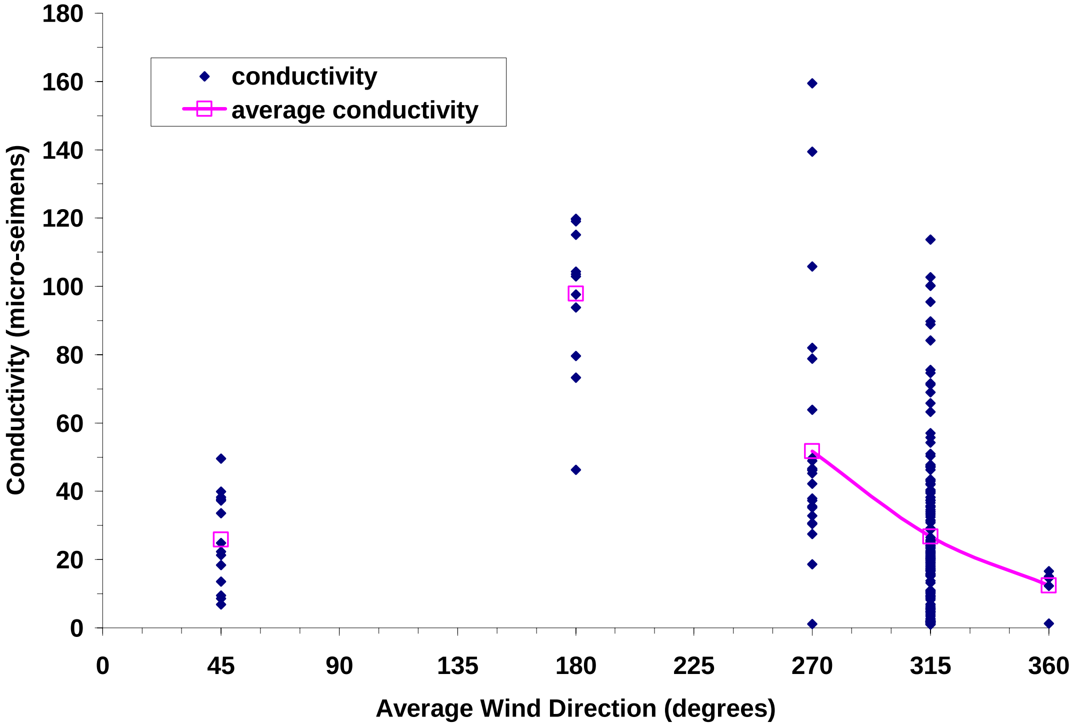

Figure 10. Conductivity vs. average wind direction of 96-hour trajectories during winter of 2000-2001.

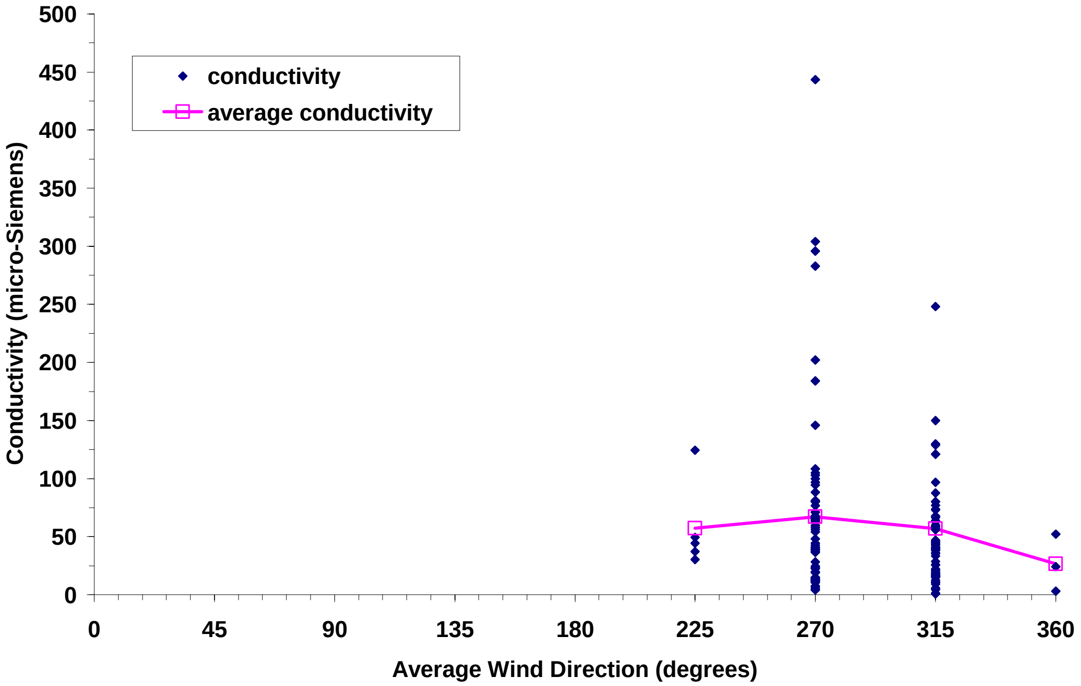

Figure 11. Conductivity vs. average wind direction of 96-hour trajectories during winter of 2001-2002.

7. DISCUSSION AND CONCLUSIONS

Measurements from 408 samples over four winters indicate that cloud water electrical conductivity varies over a wide range. Conductivities ranged from less than 1.0 μS cm^{-1} to 444 μS cm^{-1}. Figure 12 shows that the distribution is strongly positively skewed – most values are at the low end of the conductivity range measured. This suggests that any technique requiring conductivity of ice from cloud water for deicing of aircraft will be operating in a difficult environment near Mt. Washington, NH.

Though we do not detail the chemical results of the trajectory analyses here with regard to air mass trajectory exposure to sulfate sources, it is clear that water with the highest conductivities originate from primarily westerly directions. Though samples from only four winters, with the majority from only two winters, does not create a definitive climatology of winter cloud water climatology at the summit of Mt. Washington, it does provide a characterization of the conductivity environments that might be encountered by aircraft flying in the Northeast.

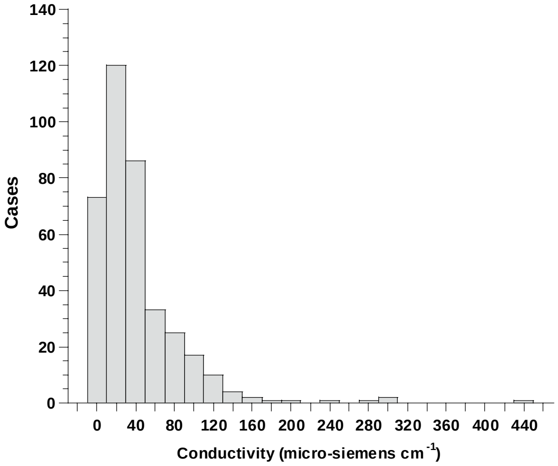

Figure 12. Conductivity measurements from four winters at the Mt. Washington Observatory.

8. ACKNOWLEDGMENTS

The authors appreciate the assistance of K. Rancourt and summit observers of Mount Washington Observatory for ice collection, and M. Twickler and S. Whitlow of the University of New Hampshire Climate Change Research Center for chemical analysis of the ice samples. We also thank A. Griffith of ERDC-CRREL for database assistance. This research is in response to requirements and funding by the FAA through the Center for Wind, Ice, and Fog Research (CWIFR). Views expressed are those of the authors and do not necessarily represent the official policy or position of the FAA or of the Army.

9. REFERENCES

Anderson, J. B., R. E. Baumgardner, V. A. Mohnen, and J. J. Bowser, 1999: Cloud chemistry in the Eastern United States, as sampled from three high-elevation sites along the Appalachian Mountains. *Atmospheric Environment*, **33**, 5105-5114.

Borys, R.D., E.E. Hindman, and P.J. Demott, 1988: The chemical fractionation of atmospheric aerosol as a result of snow crystal formation and growth. *Journal of Atmospheric Chemistry*, **7**, 213-239.

Cini, R., F. Prodi, G. Santachiara, F. Porcu, S. Bellandi, A.M. Stortini, C. Oppo, R. Udisti, and F. Pantani, 2002: Chemical characterization of cloud episodes at a ridge site in Tuscan Appennines, Italy. *Atmospheric Research*, **61**, 311-334.

Climate Change Research Center, 1998: New England's changing climate, weather and air quality, University of New Hampshire, Durham, NH, 48 pp.

FAA, 1991: *Aircraft Icing Handbook.* U.S. Department of Transportation, **1**, **2**, **3**, DOT/FAA/CT-88/8-1, DTIC ADA 238 039.

Hemmerlein, M.T., and T.D. Perkins, 1993: Techniques for pollution monitoring in remote sites: III. Near real-time monitoring of cloud water conductivity and pH. *Water, Air, and Soil Pollution*, **71**, 43-50.

Petrenko, V.F., 1998: Effect of electric fields on adhesion of ice to mercury, *Journal of Applied Physics,*. **84**, No. 1, 1 July.

Petrenko, V. F., and Z. Courville, 2000: Active de-icing coating for airfoils, *Proc. 38th Aerospace Sciences Meeting and Exhibit*, AIAA 2000-0632, 10-13 January, Reno Nevada.

Petrenko, V. F., and S. Qi, 1999: Reduction of ice adhesion to stainless steel by electrolysis, *Journal of Applied Physics*, **86**, 5450-5459.